

# Divergence of the Grüneisen Ratio at Quantum Critical Points in Heavy Fermion Metals

R. Küchler,<sup>1</sup> N. Oeschler,<sup>1</sup> P. Gegenwart,<sup>1</sup> T. Cichorek,<sup>1</sup> K. Neumaier,<sup>2</sup> O. Tegus,<sup>3</sup> C. Geibel,<sup>1</sup> J. A. Mydosh,<sup>1,4</sup>  
F. Steglich,<sup>1</sup> L. Zhu,<sup>5</sup> and Q. Si<sup>5</sup>

<sup>1</sup>Max-Planck Institute for Chemical Physics of Solids, D-01187 Dresden, Germany

<sup>2</sup>Walther Meissner Institute, D-85748 Garching, Germany

<sup>3</sup>Van der Waals-Zeeman Laboratory, University of Amsterdam, The Netherlands

<sup>4</sup>Kamerlingh Onnes Laboratory, Leiden University, The Netherlands

<sup>5</sup>Department of Physics and Astronomy, Rice University, Houston, Texas 77005-1892, USA

(Received 28 February 2003; published 5 August 2003)

We present low-temperature volume thermal expansion,  $\beta$ , and specific heat,  $C$ , measurements on high-quality single crystals of  $\text{CeNi}_2\text{Ge}_2$  and  $\text{YbRh}_2(\text{Si}_{0.95}\text{Ge}_{0.05})_2$  which are located very near to quantum critical points. For both systems,  $\beta$  shows a more singular temperature dependence than  $C$ , and thus the Grüneisen ratio  $\Gamma \propto \beta/C$  diverges as  $T \rightarrow 0$ . For  $\text{CeNi}_2\text{Ge}_2$ , our results are in accordance with the spin-density wave (SDW) scenario for three-dimensional critical spin fluctuations. By contrast, the observed singularity in  $\text{YbRh}_2(\text{Si}_{0.95}\text{Ge}_{0.05})_2$  cannot be explained by the itinerant SDW theory but is qualitatively consistent with a locally quantum critical picture.

DOI: 10.1103/PhysRevLett.91.066405

PACS numbers: 71.10.Hf, 71.27.+a

Quantum critical points (QCPs) are of extensive current interest to the physics of correlated electrons, as the proximity to a QCP provides a route towards non-Fermi liquid (NFL) behavior. While a broad range of correlated electron materials is being studied in this context, heavy fermions have been playing an especially important role: A growing list of heavy fermion (HF) metals explicitly displays magnetic QCPs [1–5]. Systematic experiments in these systems promise to shed considerable light on the general physics of quantum critical metals. Indeed, recent experiments [1,2] have shown that, at least in some of the HF metals, the traditional theory of metallic magnetic quantum phase transition fails. This traditional picture [6] describes a  $T = 0$  spin-density wave (SDW) transition and, relatedly, a mean-field-type of quantum critical behavior. More recently, it has been shown that a destruction of Kondo resonances can lead to a breakdown of the SDW picture [7,8]; what emerges instead are new classes of QCPs that are locally critical [7].

Given these experimental and theoretical developments, it seems timely to address the conditions under which these different types of QCPs arise. For this purpose, it would be important to carry out comparative studies of different heavy fermion materials. This paper reports one such study. We have chosen the HF systems  $\text{CeNi}_2\text{Ge}_2$  [4] and  $\text{YbRh}_2(\text{Si}_{0.95}\text{Ge}_{0.05})_2$  [5,9], both of which crystallize in the tetragonal  $\text{ThCr}_2\text{Si}_2$  structure. Both are ideally suited to study antiferromagnetic (AF) QCPs since they are located very near to the magnetic instability, and since the effect of disorder is minimized in these high-quality single crystals with low residual resistivities. We have focused on measurements of the thermal expansion,  $\beta$ , and Grüneisen ratio,  $\Gamma \propto \beta/C$ , where  $C$  denotes the specific heat, since recent theoretical work [10] has shown that (i)  $\Gamma$  is divergent as  $T$  goes to zero at any QCP and (ii) the associated critical expo-

nent can be used to differentiate between different types of QCP.

Presently, measurements of the thermal expansion and Grüneisen ratio for systems located directly at the QCP are lacking. Only for  $\text{Ce}_{1-x}\text{La}_x\text{Ru}_2\text{Si}_2$ , which orders antiferromagnetically for  $x > x_c$  with  $x_c = 0.075$ ,  $\beta$  has been measured for concentrations  $x = 0$  and  $x = 0.05$  at temperatures above 0.4 K. A very large  $\Gamma$  was obtained which, however, was found to saturate at low temperatures [11]. In other solids also, all previous measurements reported in the literature yield a finite Grüneisen ratio [12].

In this Letter, we communicate the first-ever observation of a divergent Grüneisen ratio  $\Gamma$  for  $T \rightarrow 0$ .  $\text{CeNi}_2\text{Ge}_2$  is known to be a NFL compound which exhibits a paramagnetic ground state [13]. The electrical resistivity,  $\rho(T)$ , resembles that of  $\text{CePd}_2\text{Si}_2$  at the pressure tuned QCP [14]:  $\rho - \rho_0 \propto T^\epsilon$  with  $1.2 \leq \epsilon \leq 1.5$  below 4 K [4,14–17]. In  $\text{YbRh}_2\text{Si}_2$ , pronounced NFL effects, i.e.,  $C/T \propto -\log(T)$  and  $\Delta\rho \sim T$ , have been observed upon cooling from 10 K down to 0.3 K. While  $\Delta\rho(T)$  keeps following the linear  $T$  dependence down to  $T_N = 70$  mK,  $C/T$  diverges stronger than logarithmically below  $T = 0.3$  K [5,18]. For our study, we chose a high-quality single crystal of  $\text{YbRh}_2(\text{Si}_{0.95}\text{Ge}_{0.05})_2$  for which  $T_N$  has been reduced to 20 mK. Large  $\text{CeNi}_2\text{Ge}_2$  single crystals of weight 5 to 6 g were grown using the traveling-floating-zone mirror-oven technique. The samples were analyzed via electron-probe microanalysis (EPMA) and found to have the desired 122 (P4/mmm) structure with little mosaic spread, good stoichiometry, and no second phases. Two thin oriented bars with a length of 5 mm were formed by spark erosion from the center of the large single crystal. The bars were annealed for 120 h at 800 °C in an Ar partial pressure (10–20 torr) and have a residual resistivity of 3–5  $\mu\Omega$  cm. Single crystalline platelets of  $\text{YbRh}_2(\text{Si}_{1-x}\text{Ge}_x)_2$  with a nominal Ge

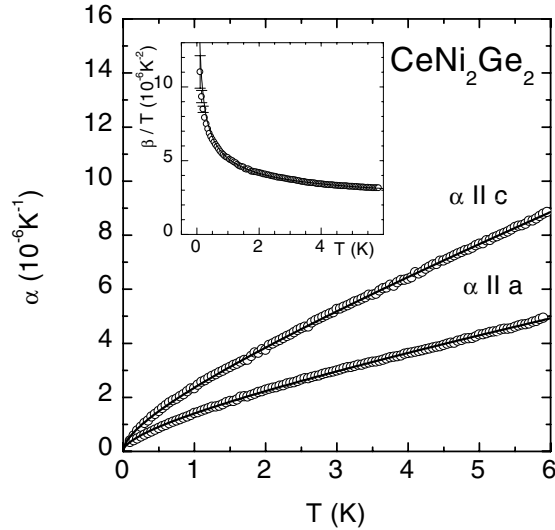


FIG. 1. Linear thermal expansions of  $\text{CeNi}_2\text{Ge}_2$  vs temperature at  $B = 0$ . The inset shows volume expansion as  $\beta/T$  vs  $T$ . Solid lines are fits as specified in Table I.

concentration of  $x = 0.05$  were grown from In flux as described earlier [5,9]. From a careful EPMA, the effective Ge concentration is found to be  $x_{\text{eff}} \leq 0.02 \pm 0.01$ . The large difference between nominal and effective Ge content is due to the fact that Ge dissolves better than Si in the In flux. A similar effective Ge content of  $0.02 \pm 0.004$  [9] is deduced from hydrostatic pressure experiments [19]. The residual resistivity of the Ge-doped crystal is  $5 \mu\Omega \text{ cm}$ . The thermal expansion and the specific heat have been determined in dilution refrigerators by utilizing an ultrahigh resolution capacitive dilatometer and the quasiadiabatic heat pulse technique, respectively.

Figure 1 displays the  $T$  dependence of  $\alpha_a$  and  $\alpha_c$ , the linear thermal expansion coefficients of  $\text{CeNi}_2\text{Ge}_2$  measured along the tetragonal  $a$  and  $c$  axes. As shown by the solid lines, the data can be described in the entire  $T$  range investigated by the  $T$  dependence predicted [10] by the three-dimensional (3D) SDW scenario, i.e., the sum of (singular) square-root and (normal) linear contributions. The corresponding fit parameters are listed in Table I. We observe a moderate anisotropy  $\alpha_c \approx 1.8\alpha_a$ . As shown in the inset, the volume expansion coefficient  $\beta = 2\alpha_a + \alpha_c$ , plotted as  $\beta(T)/T$ , is not a constant upon cooling, as would be for a Fermi liquid, but shows a  $1/\sqrt{T}$  divergence over more than two decades in temperature from 6 K down to at least 50 mK. This is one of the cleanest

observations of NFL behavior in a thermodynamic property made in any system thus far.

We next consider the low-temperature specific heat of  $\text{CeNi}_2\text{Ge}_2$ . As shown by several investigations,  $C(T)/T$  strongly increases upon cooling from 6 to 0.4 K [4,16,20–22]. This increase has either been described by  $C(T)/T \propto -\log(T)$  [4,16] or  $C(T)/T = \gamma_0 - c\sqrt{T}$  [21]. Below 0.4 K, different behaviors have been reported. While Knopp *et al.* found a peak at 0.3 K followed by a 6% decrease in  $C(T)/T$  from the maximum value [20], Koerner *et al.* observed a leveling off in  $C(T)/T$  below 0.3 K [16]. In contrast,  $C(T)/T$  of a high-quality sample with very low residual resistivity does not saturate but shows an upturn at the lowest temperatures [22]. Very recently, a systematic study of the low-temperature specific heat on different high-quality polycrystals, prepared with a slight variation of the stoichiometry [15], has been performed. The result was that nearly all of the different investigated samples showed such an upturn in  $C(T)/T$  below 0.3 K whose size, however, is strongly sample dependent even for samples with similar  $\rho(T)$  and a residual resistivity of only  $0.2 \mu\Omega \text{ cm}$  [23]. In the following, we analyze the specific heat (Fig. 2) measured on the same sample that has been used for the thermal expansion study. Below 3 K, the data can be described by  $C(T)/T = \gamma_0 - c\sqrt{T} + d/T^3$  using the parameters listed in Table I (solid lines in Fig. 2). Here we assume that the low-temperature upturn, present in this single crystal as well, could be ascribed to the high-temperature tail of a Schottky anomaly [25]. Its influence on the Grüneisen ratio is smaller than 5% at 0.1 K and therefore not visible in the  $\Gamma(T)$  plot shown in the inset of Fig. 2. This is the first observation of a divergent  $\Gamma(T)$  for  $T \rightarrow 0$  in any material and provides striking evidence that  $\text{CeNi}_2\text{Ge}_2$  is located very close to a QCP. The observed  $T$  dependence is in full agreement with the 3D SDW prediction [10]. If the investigated high-quality single crystal would enter a Fermi liquid regime below 0.3 K as observed for the sample studied in [16],  $\Gamma(T)$  should saturate below that temperature.

The application of magnetic fields to  $\text{CeNi}_2\text{Ge}_2$  is found to gradually reduce the low- $T$  specific heat coefficient. For  $B \geq 2 \text{ T}$ , a nearly temperature-independent  $\gamma(B) = C(T, B)/T$  is observed at low temperatures with  $\gamma(B) = \gamma_0 - \text{const}\sqrt{B}$  [21]. The low-temperature thermal expansion shows a similar field-induced crossover to Fermi liquid behavior (Fig. 3) and the field dependence of  $\alpha(T, B)/T$  in the field-induced FL regime diverges

TABLE I. Fit forms and parameters for  $\text{CeNi}_2\text{Ge}_2$ .

$\alpha(T) = a\sqrt{T} + bT$	$\alpha \parallel c$	$a = 1.5 \times 10^{-6} \text{ K}^{-1.5}, b = 0.87 \times 10^{-6} \text{ K}^{-2}$
$\beta(T) = a\sqrt{T} + bT$	$\alpha \parallel a$	$a = 0.99 \times 10^{-6} \text{ K}^{-1.5}, b = 0.42 \times 10^{-6} \text{ K}^{-2}$
$C(T)/T = \gamma_0 - c\sqrt{T} + d/T^3$	$\beta$	$a = 3.5 \times 10^{-6} \text{ K}^{-1.5}, b = 1.7 \times 10^{-6} \text{ K}^{-2}$
		$\gamma_0 = 0.46 \text{ JK}^{-2} \text{ mol}^{-1}, c = 0.11 \text{ Jmol}^{-1} \text{ K}^{-5/2}$
		$d = 102 \mu\text{J Kmol}^{-1}$

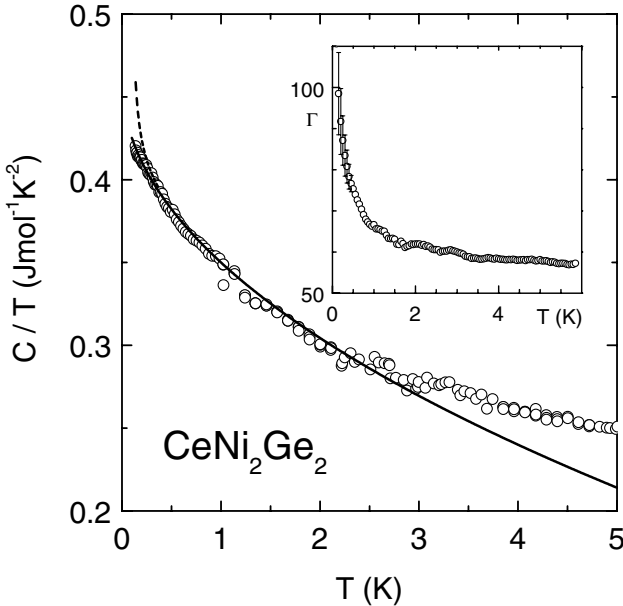


FIG. 2. Specific heat at  $B = 0$  as  $C/T$  vs  $T$  for  $\text{CeNi}_2\text{Ge}_2$ . From the raw data (dashed line at low  $T$ ), a contribution  $C_n = \alpha/T^2$  with  $\alpha = 102 \mu\text{J K/mol}$  has been subtracted giving the low- $T$  open circles. The inset shows the  $T$  dependence of the Grüneisen ratio  $\Gamma = V_m/\kappa_T \cdot \beta/C$ , where  $V_m$  and  $\kappa_T$  are the molar volume and isothermal compressibility, respectively. Here, we use  $\kappa_T = 1.15 \times 10^{-11} \text{ Pa}^{-1}$  as determined from high-pressure lattice parameter measurements at room temperature [24]. The solid line is a fit as specified in Table I.

similar to  $1/\sqrt{B}$  (not shown). Both features are consistent with the predictions [10] from the itinerant 3D SDW fluctuations at a zero-field AF QCP, assuming a linear dependence between the magnetic field and the distance  $r$  from the QCP.

We now turn to  $\text{YbRh}_2(\text{Si}_{0.95}\text{Ge}_{0.05})_2$ , in which we have measured the thermal expansion from 50 mK to 6 K. Compared to  $\text{CeNi}_2\text{Ge}_2$ , here the volume thermal expansion coefficient  $\beta(T)$  has an opposite sign reflecting the opposite volume dependence of the characteristic energies. At  $T > 1 \text{ K}$ ,  $\beta(T)$  can be fit by  $-T \log(T_0/T)$  with  $T_0 \approx 13 \text{ K}$  (see Fig. 4). At  $T < 1 \text{ K}$ , the best fit is given by  $a_1 + a_0 T$ . Both are not only different from the expected 3D-SDW results discussed earlier, but also weaker than the  $\ln \ln T$  form [10] expected in a 2D-SDW picture [27]. The difference from the 2D-SDW picture is even more striking when we look at the Grüneisen ratio. In Fig. 4, we have also shown the electronic specific heat at zero magnetic field. Here  $C_{el} = C - C_Q$ , where  $C_Q \propto 1/T^2$  denotes the nuclear quadrupolar contribution determined from recent Mössbauer results [26]. At 20 mK, a maximum in  $C_{el}(T)/T$  marks the onset of very weak AF order [9]. This is suppressed by a tiny critical magnetic field of  $B_c = 0.027 \text{ T}$  applied in the easy plane. At  $B = B_c$ , a power law divergence  $C_{el}(T)/T \propto T^{-1/3}$  is observed (which is already incompatible with the 2D-SDW picture) [9]. At higher temperatures, the zero-field specific heat coefficient also varies as  $\log(T'_0/T)$  with  $T'_0 = 30 \text{ K}$

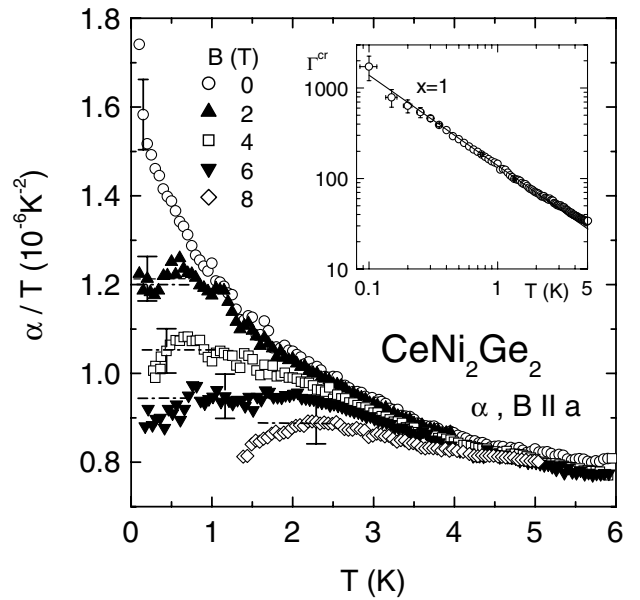


FIG. 3. Thermal expansion of  $\text{CeNi}_2\text{Ge}_2$  along the  $a$  axis as  $\alpha/T$  vs  $T$  at varying magnetic fields. The inset shows the critical Grüneisen ratio  $\Gamma^{cr} = V_m/\kappa_T \cdot \beta^{cr}/C^{cr}$  as  $\log \Gamma^{cr}$  vs  $\log T$  (at  $B = 0$ ) with  $\beta^{cr} = \beta(T) - bT$  and  $C^{cr} = C(T) - (\gamma T + d/T^2)$  using the parameters listed in Table I. The solid line represents  $\Gamma^{cr} \propto 1/T^x$  with  $x = 1$ .

(Fig. 4) [5]. Because of the difference between  $T'_0$  and  $T_0$ , the Grüneisen ratio is strongly temperature dependent. Below 1 K, it diverges as  $\Gamma(T) = \Gamma_0 + cT^{-2/3}$ , i.e., weaker than the  $\frac{1}{T} \frac{\ln \ln(T)}{\ln(T)}$  form expected in a 2D-SDW

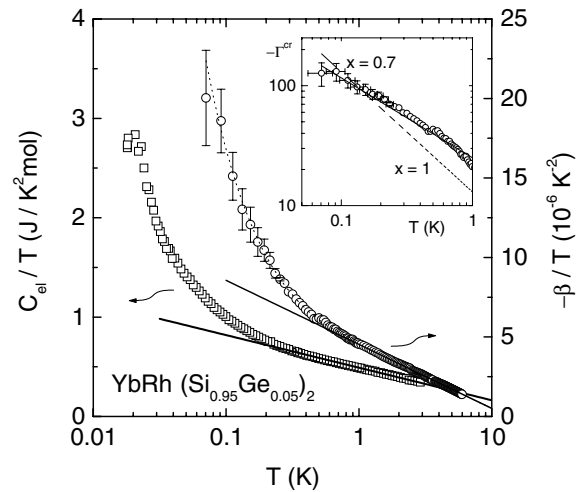


FIG. 4. Electronic specific heat as  $C_{el}/T$  (left axis) and volume thermal expansion as  $-\beta/T$  (right axis) vs  $T$  (on a logarithmic scale) for  $\text{YbRh}_2(\text{Si}_{0.95}\text{Ge}_{0.05})_2$  at  $B = 0$ . The solid lines indicate  $\log(T_0/T)$  dependences with  $T_0 = 30 \text{ K}$  and  $13 \text{ K}$  for  $C_{el}/T$  and  $-\beta/T$ , respectively. The dotted line represents  $-\beta/T = a_0 + a_1/T$  with  $a_0 = 3.4 \times 10^{-6} \text{ K}^{-2}$  and  $a_1 = 1.34 \times 10^{-6} \text{ K}^{-1}$ . The inset displays the log-log plot of  $\Gamma^{cr}(T)$  with  $\Gamma^{cr} = V_m/\kappa_T \cdot \beta^{cr}/C^{cr}$  using  $\kappa_T = 5.3 \times 10^{-12} \text{ Pa}^{-1}$  [26],  $\beta^{cr} = \beta(T) + a_0 T$ , and  $C^{cr} = C_{el}(T)$ . The solid and dotted lines represent  $\Gamma^{cr} \propto 1/T^x$  with  $x = 0.7$  and  $x = 1$ , respectively.

picture [10]. We note that, in the measured temperature range, the zero-field data of both the specific heat and thermal expansion are identical to their counterparts at the critical magnetic field.

To interpret our results, we introduce a Grüneisen exponent  $x$  in terms of the critical Grüneisen ratio  $\Gamma^{cr} \propto \beta^{cr}/C_V^{cr} \propto 1/T^x$ , where  $\beta^{cr}$  and  $C_V^{cr}$  are the thermal expansion and specific heat with the background contributions subtracted; this exponent is equal to the dimension of the most relevant operator that is coupled to pressure [10]. It is shown in Ref. [7] that, for magnetically three-dimensional systems without frustration, the SDW picture should apply. This is consistent with our finding here that both the thermal expansion and specific heat results in CeNi<sub>2</sub>Ge<sub>2</sub> can be fit by the respective expressions for a 3D-AF-SDW theory [28]. Our results correspond to  $\beta^{cr} \propto \sqrt{T}$  and  $C_V^{cr} \propto T^{3/2}$ , leading to  $\Gamma_{cr} \propto \frac{1}{T}$ . In other words, the Grüneisen exponent  $x = 1$  (with error bars  $+0.05/-0.1$ , as determined from a log-log plot shown in the inset of Fig. 3). In an SDW picture, the most relevant term is the quadratic part of the  $\phi^4$  theory. The corresponding dimension is  $1/\nu z = 1$ , where the spatial-correlation-length exponent  $\nu = 1/2$  and the dynamic exponent  $z = 2$ .

For YbRh<sub>2</sub>(Si<sub>1-x</sub>Ge<sub>x</sub>)<sub>2</sub>, on the other hand, the measured Grüneisen exponent is fractional:  $x = 0.7 \pm 0.1$  as determined from a log-log plot of  $\Gamma^{cr}$  versus temperature shown in the inset of Fig. 4. While definitely not compatible with the itinerant SDW theory, a fractional Grüneisen exponent is consistent with the locally quantum critical point. One kind of condition favorable for this new type of QCP corresponds to a magnetic fluctuation spectrum that is strongly anisotropic [7]. At such a locally quantum critical point, spatially local critical excitations emerge and coexist with the spatially extended critical spin fluctuations. There are then two scaling dimensions to be considered. For the tuning of the long-wavelength fluctuations, the dimension of interest is still given by the expression  $1/\nu z$ . While  $\nu$  remains  $1/2$ , the dynamic exponent  $z$  becomes  $2/\alpha > 2$  where  $\alpha$  is the fractional exponent that characterizes the dynamical spin susceptibility. As a result,  $1/\nu z < 1$ . For the tuning of the local fluctuations, the corresponding dimension is the inverse of the temporal-correlation-length exponent. Within an  $\epsilon$  expansion scheme as carried out in Ref. [29] and for the XY-spin-invariant case of relevance to YbRh<sub>2</sub>(Si<sub>1-x</sub>Ge<sub>x</sub>)<sub>2</sub>, this exponent is found [30] to be 0.62 to the first order in  $\epsilon$  and 0.66 to the second order in  $\epsilon$ . The overall Grüneisen ratio will then display a fractional exponent, as indeed seen experimentally.

We are grateful to M. Lang, O. Trovarelli, and H. Wilhelm for valuable conversations, F. Weickert and J. Custers for their help with the resistivity experiments, and the Fonds der Chemischen Industrie (Dresden), the

Dutch Foundation FOM-ALMOS (O.T. and J.A.M.), NSF, TCSAM, and Robert A. Welch Foundation (L.Z. and Q.S.) for support.

- 
- [1] G. R. Stewart, Rev. Mod. Phys. **73**, 797 (2001).
  - [2] A. Schröder *et al.*, Nature (London) **407**, 351 (2000).
  - [3] N. D. Mathur *et al.*, Nature (London) **394**, 39 (1998).
  - [4] P. Gegenwart *et al.*, Phys. Rev. Lett. **82**, 1293 (1999).
  - [5] O. Trovarelli *et al.*, Phys. Rev. Lett. **85**, 626 (2000).
  - [6] S. Sachdev, *Quantum Phase Transitions* (Cambridge University Press, Cambridge, England, 1999), Chap. 12.
  - [7] Q. Si *et al.*, Nature (London) **413**, 804 (2001).
  - [8] P. Coleman *et al.*, J. Phys. Condens. Matter **13**, R723 (2001).
  - [9] J. Custers *et al.*, Nature (London) **424**, 524 (2003).
  - [10] L. Zhu *et al.*, preceding Letter, Phys. Rev. Lett. **91**, 066404 (2003).
  - [11] S. Kambe *et al.*, J. Phys. Condens. Matter **9**, 4917 (1997).
  - [12] P. Thalmeier and B. Lüthi, *Handbook on the Physics and Chemistry of Rare Earths*, edited by K. A. Gschneider, Jr. and L. Eyring (Elsevier, Amsterdam, 1991), Vol. 14, p. 225.
  - [13] A superconducting transition, observed below 0.2 K in some electrical resistivity measurements [14–17], has not been detected by any bulk probe thus far.
  - [14] F. M. Grosche *et al.*, J. Phys. Condens. Matter **12**, L533 (2000).
  - [15] P. Gegenwart *et al.*, Physica (Amsterdam) **281B&282B**, 5 (2000).
  - [16] S. Koerner *et al.*, J. Low Temp. Phys. **119**, 147 (2000).
  - [17] D. Braithwaite *et al.*, J. Phys. Condens. Matter **12**, 1339 (2000).
  - [18] P. Gegenwart *et al.*, Phys. Rev. Lett. **89**, 056402 (2002).
  - [19] S. Mederle *et al.*, J. Phys. Condens. Matter **14**, 10731 (2002).
  - [20] G. Knopp *et al.*, J. Magn. Magn. Mater. **74**, 341 (1988).
  - [21] Y. Aoki *et al.*, J. Phys. Soc. Jpn. **66**, 2993 (1997).
  - [22] F. Steglich *et al.*, Physica (Amsterdam) **341C–348C**, 691 (2000).
  - [23] T. Cichorek *et al.*, Acta Phys. Pol. B **34**, 371 (2003).
  - [24] T. Fukuhara *et al.*, Physica (Amsterdam) **230B–232B**, 198 (1997).
  - [25] The upturn is not a part of the quantum critical behavior: It remains in a magnetic field of about 2 T which, at  $T < 0.7$  K, is outside the quantum critical regime: T. Cichorek *et al.* (to be published).
  - [26] J. Plessel *et al.*, Phys. Rev. B **67**, 180303 (2003).
  - [27] The data for  $T < 1$  K allow a fitting with  $a_1 + a_0 T + a_2 \ln(\ln(T_0/T))$  [10], but the extracted  $\ln(\ln(T_0/T))$  component is negligible compared to the other terms.
  - [28] Recent neutron scattering measurements indeed show that the low energy magnetic fluctuation spectrum in CeNi<sub>2</sub>Ge<sub>2</sub> is 3D: H. Kadowaki *et al.*, Acta Phys. Pol. B **34**, 375 (2003).
  - [29] L. Zhu and Q. Si, Phys. Rev. B **66**, 024426 (2002).
  - [30] L. Zhu and Q. Si (unpublished).